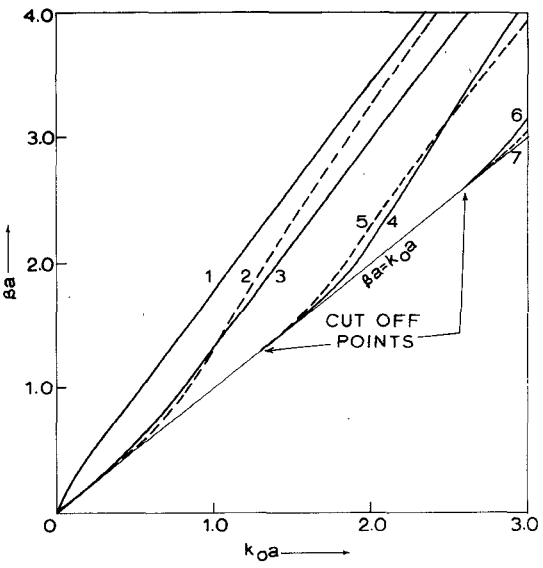

Fig. 3. Dispersion characteristics of a normal helix for $\varepsilon_r = 2.56$ and $\alpha = 60°$. Continuous lines represent even modes and dotted lines odd modes.

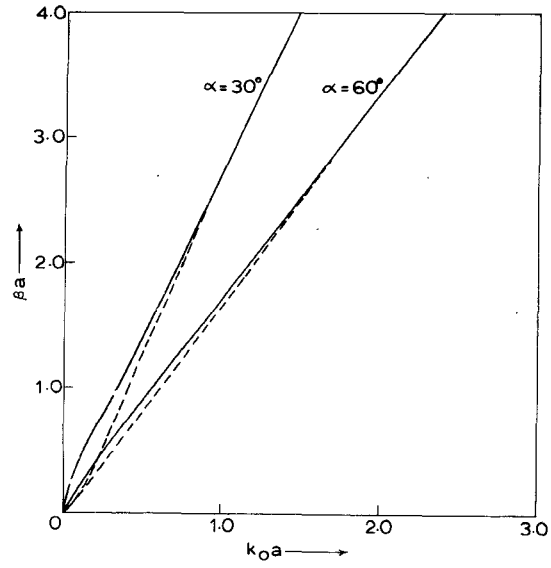

Fig. 4. Dispersion characteristics of an inverted helix for $\varepsilon_r = 2.56$. Continuous lines represent even modes and dotted lines odd modes.

have low-frequency cutoffs given by

$$k_{0c}a = \frac{n\pi}{2(\varepsilon_r - 1)^{1/2}}, \qquad n = 1,2,3,\cdots. \tag{3}$$

At these cutoff frequencies, u_0 vanishes; correspondingly, $\beta = k_{0c}$. It is observed that the curves for modes 1 and 2 tend to merge at higher frequencies. These modes correspond to the two modes which exist when medium 2 also is air [2]. Mode 3, unlike modes 1 and 2, does not have a counterpart in the air case and arises because of the dielectric. Similarly, the presence of higher order modes is also attributed to the dielectric. This conclusion is substantiated by the fact that the modes of the dielectric have cutoff frequencies which also are given by (3) [4].

B. Inverted Helix

In the case of an inverted helix, one sets $\varepsilon_2 = \varepsilon_0$, $\varepsilon_1 = \varepsilon_r\varepsilon_0$, $k_2 = k_0$, $u_2 = u_0$ in (1) and (2). Since, from (2), $u_0^2 = u_1^2 + k_0^2(\varepsilon_r - 1)$ and $u_1 > 0$, $\varepsilon_r > 1$, u_0 is always positive real. Hence there are no modes having trigonometric variation in the central (air) region. A study of the characteristic equations shows that there are only two roots, one symmetric and the other antisymmetric, neither of which has a cutoff frequency. The phase constants are depicted in Fig. 4 as functions of k_0a. These modes are akin to those that exist on a pair of unidirectionally conducting screens in free space [2].

It may be noted that both in the case of normal and inverted helices, there is a single transverse-antisymmetric mode that has no cutoff frequency. By a proper choice of excitation, symmetric modes may be eliminated [3], and the guide dimensions may be chosen in such a way that unimodal propagation occurs.

The electromagnetic field in all the modes is, in general, elliptically polarized both in the longitudinal (xz) and transverse (xy) planes. Further, in all the cases, $E_{y'}$ vanishes in the entire region $x \geq a$ and $E_{y''}$ vanishes in the entire region $x \leq -a$. In the sandwiched region, the electric field vanishes in directions making angles θ_s and θ_a with the y axis for the symmetric and antisymmetric cases, respectively, where these angles are given by

$$\begin{matrix}\theta_s \\ \theta_a\end{matrix} = \tan^{-1}\left(\tan\alpha \begin{matrix}\tanh \\ \coth\end{matrix} u_2a \begin{matrix}\coth \\ \tanh\end{matrix} u_2x\right). \tag{4}$$

In the plane $x = 0$, $\theta_s = \pi/2$, and $\theta_a = 0$. Thus even and odd modes may be distinguished by the manner in which the direction of vanishing electric field component turns while passing from the top to the bottom screen.

Conclusion

A modal analysis has been carried out for the normal and inverted flattened sheath helices. It is shown that by proper geometry and excitation scheme, propagation in a single mode can be assured. The slow wave and polarization properties suggest useful applications for such planar structures. For example, the polarization characteristics may be utilized to fabricate nonreciprocal ferrite components.

References

[1] D. A. Watkins, *Topics in Electromagnetic Theory*. New York: John Wiley, 1958.
[2] R. K. Arora, "Surface waves on a pair of parallel unidirectionally conducting screens," *IEEE Trans. Antennas Propagat.*, vol. AP-14, pp. 795–797, Nov. 1966.
[3] ——, "Field of a line source situated parallel to a surface-wave structure comprising a pair of unidirectionally conducting screens," *Can. J. Phys.*, vol. 45, pp. 2145–2172, June 1967.
[4] R. E. Collin, *Field Theory of Guided Waves*. New York: McGraw-Hill, 1960, pp. 470–474.

Influence of Spatial Dispersion of the Shield Transfer Impedance of a Braided Coaxial Cable

J. R. WAIT AND D. A. HILL

***Abstract*—The effect of the dependence of the braid transfer impedance on the propagation constant is discussed for a coaxial cable located in a circular tunnel.**

In recent papers [1], [2] in this TRANSACTIONS, we have presented attenuation calculations for a braided coaxial cable located within a circular tunnel bounded by a homogeneous

Manuscript received May 4, 1976.
J. R. Wait is with the Cooperative Institute for Environmental Sciences, University of Colorado, Boulder, CO 80309.
D. A. Hill is with the Office of Telecommunications, Institute for Telecommunication Sciences, U.S. Department of Commerce, Boulder, CO 80302.

lossy medium. Following previous engineering practice, the metal braid was represented by a transfer impedance Z_T that was assumed not to vary with the propagation constant of the desired mode. In fact, for the calculations, we assumed that $Z_T = i\omega L_T$ where L_T was the transfer inductance expressed in nanohenries per meter. But this is a limitation in the calculations, not in the theoretical formulation.

Recent theoretical work [3]–[5] on wire mesh screens suggests that the effective transfer impedance is better represented by the form

$$Z_T = A(\omega) + B(\omega)\Gamma^2 \tag{1}$$

where $A(\omega)$ and $B(\omega)$ are frequency-dependent parameters that do not depend on the propagation constant Γ. In the specific case of the uncoated braided coaxial cable model used earlier, we would have

$$Z_T = i\omega L_T[1 + \Gamma^2/(k_0^2 + k^2)] \tag{2}$$

where k_0 is the wave number for the region (i.e., air) adjacent to the cable and k is the wave number for the insulating dielectric on the inside of the shield. This particular form would apply if the weave or pitch angle ψ of the braid wires (angle subtended with the cable axis) is 45° and if the axial separation of the braid wires is small compared with a wavelength and with the radius of the shield. Of course, the formula, but not the form, for Z_T is modified if other factors are considered, such as the influence of the jacket material and any external lossy coatings. Also, if the weave angle is different from 45°, we should replace the bracketed term in (2) by $[1 + (2\Gamma^2 \cos^2 \psi)/(k_0^2 + k^2)]$ according to an analysis by Casey [5].

The general mode equations [1], [2] we have derived for the braided cable in the tunnel may still be used if Z_T is regarded to be Γ dependent. The iterative calculation is only slightly more complicated. However, it is useful to examine how much error is incurred by adopting an appropriate Γ-independent model for Z_T since this has been used frequently in the past. For the coaxial cable or bifilar mode, Γ is of the order of ik; thus we propose to use the approximation

$$Z_T(\Gamma) \simeq Z_T(ik) = i\omega L_T(1 - k^2/(k_0^2 + k^2)]$$
$$= i\omega L_T k_0^2/(k_0^2 + k^2). \tag{3}$$

The limiting case is obtained by setting $\Gamma = 0$ in (2). Then we recover the simple form $Z_T \simeq i\omega L_T$.

To illustrate the significance of the present results, we plot in Figs. 1–3 the attenuation rate of the bifilar mode in decibels per kilometer for the three cases mentioned previously. Specifically, the transfer impedance takes the respective forms $Z_T(\Gamma)$, $Z_T(ik)$, and $Z_T(0)$ as indicated on each figure.

The cable parameters, in terms of the earlier notation [1], [2], are a_0 (tunnel radius) = 2 m, σ_e (earth conductivity) = 10^{-3} mhos/m, $\varepsilon_e/\varepsilon_0 = 10$, a (inner conductor radius) = 1.5 mm, b (sheath radius) = 10 mm, $\varepsilon/\varepsilon_0$ (dielectric constant of insulator) = 1.5, and σ_w (conductivity of inner conductor) = 5.7×10^7 mhos/m. Also, as mentioned previously, the influence of the jacket and/or lossy external layer is ignored here. This corresponds to setting $c = b$ and $\sigma d = 0$ in the previous formulation [1], [2]. As indicated in the figures, ρ_0 (offset distance of cable from tunnel axis) is either zero or $0.9a_0 = 1.8$ m. In Fig. 1, where the reference value of L_T is 40 nH/m, it is seen that the attenuation rates for $Z_T(\Gamma)$ and $Z_T(ik)$ are considerably lower than that for $Z_T(0)$. In Fig. 2, where $L_T = 10$ nH/m, the difference is somewhat reduced, while in Fig. 3 where $L_T = 2$ nH/m, the difference is negligible. In all cases shown the difference between the curves for $Z_T(\Gamma)$ and $Z_T(ik)$ would seem to be insignificant.

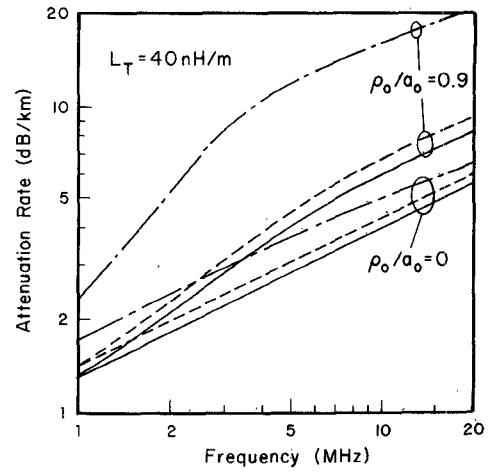

Fig. 1. Attenuation rate of a braided coaxial cable in a circular tunnel for three different representations of the sheath transfer impedance. The reference transfer inductance L_T is 40 nH/m. $Z_T(0)$: — - — -. $Z_T(ik)$: - - - - -. $Z_T(\Gamma)$: ————.

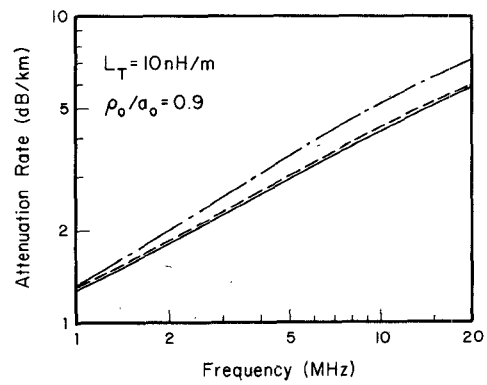

Fig. 2. Attenuation rate of a braided coaxial cable in a circular tunnel for three different representations of the sheath transfer impedance. The reference transfer inductance is $L_T = 10$ nH/m. $Z_T(0)$: — - — -. $Z_T(ik)$: - - - - -. $Z_T(\Gamma)$: ————.

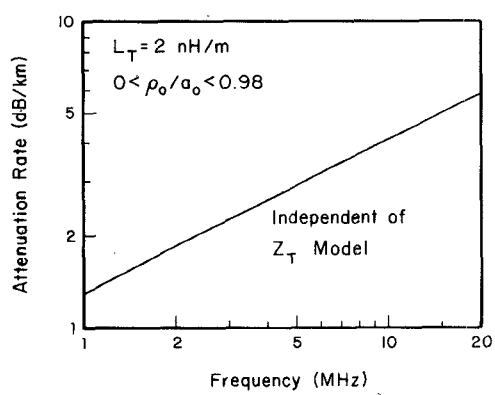

Fig. 3. Attenuation rate of a braided coaxial cable in a circular tunnel for three different representations of the sheath transfer impedance. The reference transfer inductance is $L_T = 2$ nH/m. Curves are indistinguishable.

Certainly from a practical standpoint, the use of an effective Γ-independent value of the transfer impedance such as $Z_T(ik)$ would lead to a negligible error. But, of course, the use of $Z_T(0)$ as may be obtained from a static test measurement is liable to produce significant discrepancies. Thus in interpreting the

calculated data from previous attenuation calculations [1], [2], one should identify the given sheath transfer impedance as an effective value for that mode (e.g., $Z_T(ik)$ for the bifilar mode and $Z_T(ik_0)$ for the monofilar mode).

Using the method discussed recently by the authors [6], the influence of the Γ dependence on Z_T on the excitation factor of the desired bifilar mode was investigated. The results showed that the ratio of the excitation factor for the $Z_T(0)$ assumption was typically 6 dB higher than for either the $Z_T(\Gamma)$ or $Z_T(ik)$ assumptions. This is not surprising since the cable is less leaky in the latter cases. To some extent, this compensates for the decreased attenuation rates insofar as the total system loss is concerned. The important point is that the excitation factors calculated for an effective $Z_T(ik)$ never differ more than 2 dB from the Γ-dependent form $Z_T(\Gamma)$ (even for the worst case where $L_T = 40$ nH/m).

Not surprisingly, the calculated transmission characteristics for such problems will depend on the many details of the assumed model. The large number of parameters, even in such an idealized configuration, makes it extremely difficult to form a comprehensive picture of the overall phenomena. Nevertheless, it appears highly worthwhile to develop engineering design criteria that can be used to estimate system performance. Work on this subject continues.

References

[1] J. R. Wait and D. A. Hill, "Propagation along a braided coaxial cable in a circular tunnel," *IEEE Trans. Microwave Theory Tech.*, vol. MTT-23, pp. 401–405, May 1975.

[2] D. A. Hill and J. R. Wait, "Propagation along a braided coaxial cable located close to a tunnel wall," *IEEE Trans. Microwave Theory Tech.*, to be published.

[3] M. I. Astrakhan, "Reflecting and screening properties of plane wire grids," *Radio Engr.* (USSR), vol. 23, pp. 76–83, Jan. 1968.

[4] D. A. Hill and J. R. Wait, "EM scattering of an arbitrary plane wave by a wire mesh with bonded junctions," *Can. J. Phys.*, vol. 54, pp. 353–361, Feb. 15, 1976.

[5] K. F. Casey, private communication, Kansas State University, 1975.

[6] D. A. Hill and J. R. Wait, "Calculated transmission loss for a leaky feeder communication system in a circular tunnel," *Radio Sci.*, vol. 11, pp. 315–322, Apr. 1976.

MIC Coupler with Improved Directivity Using Thin-Film Bi_2O_3 Overlay

R. N. KAREKAR AND MADAN K. PANDE

***Abstract*—Results of the effect of thin-film Bi_2O_3 overlay on a directional coupler at X band are reported. Directivity between 14 and 23 dB was obtained over the band.**

The results obtained with a 12-dB directional coupler during the investigations on 3-layer microstrip, utilizing thin-film oxide overlay, are described. Fig. 1 gives the sketch of the directional coupler showing the type of the overlay employed.

Alumina substrates (0.025 × 1 × 1 in) metallized with 200 Å of chromium, 1000 Å of nickel and 3 μm of gold were used for this study. A 12-dB directional coupler was designed ($f_0 = 9.23$ GHz, $Z_0 = 50\ \Omega$) using data from the papers of Schwarzmann [1], Bryant and Weiss [2], and Wheeler [3]. A 3-percent undercut was allowed in the negative design. Care was taken to keep the uncoupled lengths from each port to the coupled region

Manuscript received February 10, 1976; revised May 5, 1976.
The authors are with the Department of Physics, University of Poona, Ganeshkhind, Poona, India.

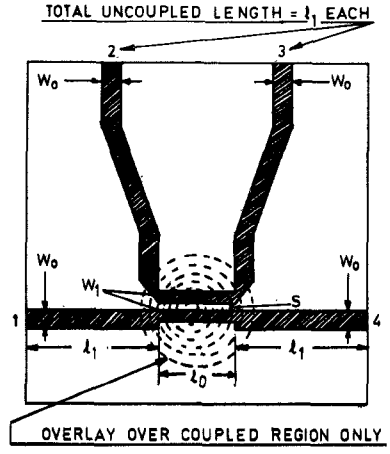

Fig. 1. Sketch of 12-dB directional coupler. Pre-etch geometry, $W_0 = 0.654$ mm, $W_1 = 0.619$ mm, $s = 0.3$ mm, $l_0 = 3.19$ mm.

the same (l_1), and to avoid performance degradation by reflections and mismatches at the transitions and the loads. At X band these port lengths reach the order of $\lambda g/4$ or more. Substrates with photolithographically delineated circuits were mounted in the vacuum deposition unit using masks which exposed mainly the coupled region to the Bi vapor stream. Bi_2O_3 overlay was obtained following the technique reported earlier [4], and based on our previous experience, the thickness of the overlays were chosen to be around 4000 and 9000 Å. The circuits were mounted on an MIC test fixture and connected to a Hewlett-Packard X-band sweep setup, using OSM transitions. The isolated port 3 was terminated with an OSM 50-Ω load cum launcher combination. On the other terminated port a precision OSM/HP 50-Ω coaxial load was used. Transmission measurements from ports 1–2, 1–4, and 1–3 were taken. A number of measurements were conducted to eliminate errors likely to be caused by imperfections of transitions and loads. The TDR display of the OSM launchers showed a resistive match; however, the loss due the use of the two OSM launchers was estimated to be about 0.5 dB. The readings without overlay have been obtained after stripping the oxide layer with dilute HCl. This was done to take into account change, if any, in metallization characteristics likely to be caused due to heat cycling.

The results of the transmission measurements are plotted in Fig. 2 for Bi_2O_3 overlays, along with the readings without overlay. The curves in Fig. 2 show negligible change in forward transmission (ports 1–4) and coupling (ports 1–2) with overlay. The isolation curve (ports 1–3) without overlay reflects a variation in directivity from 11 dB at 8.5 GHz to 4 dB at 12 GHz. A 1-dB increase in directivity throughout this frequency range was obtained with Bi_2O_3 overlay thickness of 3900 Å. When the Bi_2O_3 overlay thickness was increased to 8500 Å, the directivity increased to 23 dB at 8.5 GHz, gradually falling to 14.5 dB at 12 GHz. The isolation curves are approximately parallel to each other. Unfortunately, no return-loss measurements could be taken for want of a coaxial dual directional coupler.

It is of interest to note that in most bulk overlays [5]–[6], the thicknesses used are of the order of 0.125–2 H (where H is the substrate thickness) and it results in a directivity of 20 dB or more. The maximum thickness of overlay reported here is of the order 1.3×10^{-3} H. Further, this thickness is just 0.28 of the thickness of the microstrip conductors (3 μm). It is felt that negligible change in coupling, despite reasonable change in